# *Dielectric Failures Reduction in the Main Stator Cell: A Mechanical and Process Engineering Approach*

*Brian Figueroa Zayas*
*Master of Engineering in Mechanical Engineering*
*Advisor: Julio Noriega Motta, Ph.D.*
*Polytechnic University of Puerto Rico*
*Graduate Project EXPO, May 2025*

***Abstract*** *— Dielectric failures account for approximately 65% of total defects in the Main Stator Cell of an aerospace manufacturing facility. This study identifies mechanical interaction during manual forming operations as the primary root cause, rather than purely electrical phenomena. Contact mechanics analysis using the Hertzian model reveals that conventional steel pliers generate contact pressures of approximately 1.10 GPa, far exceeding enamel insulation tolerance. A dedicated Delrin forming tool reduces contact pressure by 99.5%, friction forces by 75%, and bending stress by 75.2%. Complementary process improvements—including standard work updates, dedicated dielectric test operations, and operator training—achieved a 37% reduction in Scrap, Rework, and Repair (SRR) costs and a 30% reduction in Parts Per Million (PPM) defect rate, surpassing the established 35% SRR target.*

***Key Terms:*** *Contact Mechanics, Dielectric Failure, PPM , SRR*

## INTRODUCTION

The aerospace manufacturing industry demands extremely high precision and strict compliance with engineering specifications to ensure the reliability and safety of flight-critical components. Stators, rotors, exciters, sensors, actuators, and generators are produced based on approved engineering drawings that define dimensional, electrical, and functional requirements. A significant portion of these processes rely on manual forming operations, making part handling a decisive factor in product quality [1].

Among all defect categories, dielectric failures—specifically ground and phase-to-phase faults—have emerged as the principal contributor to quality escapes and production losses. Despite their significant operational impact, no prior initiative had been exclusively dedicated to their systematic root-cause elimination. This project addresses that gap by combining contact mechanics modeling with structured manufacturing process improvement to quantify and mitigate the mechanical drivers of insulation damage [2].

The following sections present the problem context, analytical methodology, process modifications, mechanical analysis, and comparative results that together validate the effectiveness of the proposed engineering solution.

## PROBLEM STATEMENT

The high rate of dielectric failures in the Main Stator Cell produced the following operational consequences:

- Significant increase in SRR and PPM metrics (see Table 1).
- Delays affecting Manufacturing Date (DTM).
- Increased process variability.
- Reduced On-Time Delivery (OTD) performance.

Additionally, a critical quality escape occurred when a unit passed internal inspections but subsequently failed dielectric testing at the customer site. Given the aerospace application of these components and their long service life under predictive maintenance programs, such failures are unacceptable [3].

**Table 1**
**Performance Baseline and Improvement Targets**

| Metric | Baseline | Target |
|---|---|---|
| SRR (Scrap/Rework/ Repair) | $200,000 | 35% Reduction |
| PPM (Parts per million) | 622,042 | 35% Reduction |

*Note: SRR is a key performance metric measuring the financial and operational impact of quality defects within a manufacturing cell.*

## METHODOLOGY

A multidisciplinary engineering approach was adopted to address the root causes of dielectric failures. The methodology integrates manufacturing process analysis, root cause identification, and quantitative mechanical modeling to develop and validate corrective actions.

### Current State Analysis

A detailed assessment of the forming process, inspection methods, and operator practices was conducted to identify inefficiencies and sources of variation. Key areas evaluated included tooling condition, standard work compliance, and defect traceability.

### Root Cause Analysis

A Fishbone (Ishikawa) Diagram was developed during a Quality Kaizen event focused on dielectric failures. This structured analysis revealed that root causes could be grouped into three primary categories related to machines and tools, methods, and personnel. The following contributing factors were identified across these categories:

- Machine / Tools: Inadequate or non-optimized tools for forming operations.
- Methods: Standard Work (JIS) lacks critical steps and clear instructions .
- Man (People): Insufficient operator skill level in measurement and inspection techniques.

Based on these findings, three primary actionable root causes were confirmed: lack of standardized work instructions, absence of structured training programs, and ineffective tool management. The following section describes the process improvements implemented to address each root cause (see Table 2).

**Table 2**
**Current Status of Main Cell Process**

| ***Evaluated Area*** | ***Current Status*** |
|---|---|
| *Root Cause Analysis* | *Not developed* |
| *Standard Work (Forming Area)* | *Incomplete / outdated* |
| *Tool & Fixture Verification Process* | *Not implemented* |
| *Forming Training Program* | *Not available* |
| *Defect Categorization (Ground vs Phase-to-Phase)* | *Not differentiated* |

## PROCESS IMPROVEMENTS

As part of the improvement strategy, several process updates and standardization actions were implemented to enhance control and reduce dielectric failures. Operation renumbering, JIS revisions, and new dedicated operations were introduced to formalize the forming workflow.

### Operation Renumbering

To improve process flow clarity and standardization, former operations 1100, 1200, and 1300 were renumbered to 1200, 1300, and 1400, respectively.

### Standard Work Enhancements (JIS Updates)

Several key standard work updates were applied to specific operations. The changes below address the deficiencies identified during the current state analysis:

- Operation 800: Dielectric testing was removed from this operation to eliminate process overload and improve task focus.
- Operation 900: Stripping and cutting specifications were added to ensure consistency and prevent insulation damage.
- Operation 950: Brazing process defined for phases A, B, and C; vacuum step added to improve joint quality and reduce contamination risks.

### New and Modified Operations

Three new operations were introduced to formalize previously uncontrolled activities and improve defect traceability:

- Dedicated Dielectric Test Operation Created: A new operation was introduced to perform dielectric testing independently, improving traceability and control.
- Operation 1000 – Alternate Dielectric Fixture: An alternative fixture was added to increase flexibility and improve testing reliability.
- Jumper Brazing Operation: A specific operation was created to standardize jumper brazing and reduce variability.

## MECHANICAL PROBLEM ANALYSIS

From a mechanical engineering perspective, the enamel insulation damage mechanism during forming can be modeled as a solid-to-solid contact problem governed by contact mechanics, friction, and bending theory. Figure 1 presents the Free Body Diagram of the AWG 16 magnet wire subjected to forming tool forces, which motivates the quantitative analysis that follows [4].

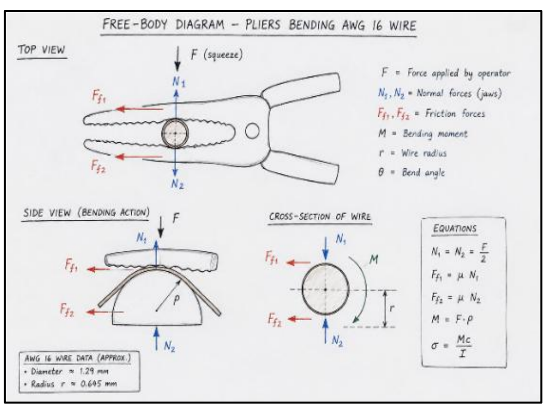


**Figure 1**
**Free Body Diagram**

### Contact Mechanics Representation

The interaction between the forming tool and the magnet wire involves three primary mechanical quantities: contact pressure distribution, friction coefficient between tool and insulation, and local deformation of the enamel layer. These are analyzed using the Hertzian contact model for cylindrical bodies [4].

The bending stress relationship is expressed as:

$$\sigma = \frac{Mc}{I} \qquad (1)$$

where:

- $\sigma$= is the bending stress
- $M$= is the applied bending moment
- $c$= is the distance from the neutral axis
- $I$= is the moment of inertia of the wire cross-section.

### Failure Mechanism

The dielectric failure mechanism is a sequential mechanical-to-electrical degradation process. Understanding the chain of events is essential for selecting the appropriate corrective intervention:

- Mechanical interaction during forming introduces localized stress concentrations in the enamel.
- Excessive pressure or friction damages the enamel coating, producing micro-cracks or thinning.
- Subsequent electrical testing or field operation induces breakdown through the damaged insulation.
- The resulting fault manifests as a dielectric failure to ground or phase-to-phase.

This analysis supports the need for tool redesign, standardized forming methods, and operator training—the three corrective pillars implemented in this project.

### Geometrical and Mechanical Properties

The following wire and tool properties were used as input to the Hertzian contact model:

- Conductor Gauge: AWG 16.
- Bare Conductor Diameter: $d_c = 1.25$ mm.
- Enamel Thickness: $t_e = 0.025$ mm.
- Total Wire Radius: $r_w = \frac{d_c}{2} + t_e = 0.625\ mm$.
- Copper Core: Young's Modulus: $E_w = 110\ GPa$.
- Poisson's Ratio: $\nu = 0.34$.

- Polished Steel tool: $E_t = 200$ GPa, $\nu_t = 0.29$.
- Friction coefficient (enamel–steel): $\mu = 0.30$.

Table 3 summarizes the mechanical advantage and jaw force comparison across different plier configurations, which establishes the applied force baseline for subsequent contact calculations.

**Table 3**
**Plier Physical Dimensions and Applied Force — Mechanical Advantage and Jaw Force Comparison**

| Tool Type | Handle Length | Jaw Length | Hand Force (N) | Jaw Force (N) |
|---|---|---|---|---|
| Standard Hand Pliers | 80 mm | 25 mm | 150 N | −480 N |
| Fine-tip Pliers | 70 mm | 15 mm | 100 N | −467 N |
| Industrial Motorized Pliers | — | — | — | 500–2000 N |

### Contact Force Calculations

Using F = 150 N at θ = 15° as representative forming conditions:

- Normal Force: N = F·cos(θ) = 150·cos(15°) ≈ 145 N
- Friction Force: $F_f = \mu N = 0.30 \times 150 = 45$ N

The equivalent elastic modulus E' = 79.24 GPa. Assuming contact length L = 5 mm, the Hertzian contact half-width b ≈ 17.37 µm. The resulting maximum contact pressure pmax ≈ 1,099 MPa (≈1.10 GPa). This pressure significantly exceeds the mechanical tolerance of enamel insulation [4], confirming the potential for micro-cracking under standard plier use.

The bending moment at the wire surface is M = Ff · rw = 45 × 0.625 = 28.13 N·mm, yielding a maximum bending stress σmax ≈ 151.6 MPa. Although calculated at the copper conductor, the enamel fails at significantly lower stress levels, making it the critical limiting factor.

## Comparative Mechanical Analysis of Forming Tools

To isolate the effect of tool geometry and material on insulation stress, two configurations were analyzed under identical loading conditions (F = 150 N, L = 5 mm, rw = 0.625 mm): Case A uses a dedicated Delrin forming tool, and Case B uses a standard general-purpose steel plier [5].

Tables 4, 5, and 6 detail the dedicated tooling geometry, tool-specific material parameters, and the resulting comparative mechanical outcomes. The combined data in Table 6 demonstrates that the Delrin tool fundamentally changes the stress state at the wire-tool interface.

**Table 4**
**Dedicated Delrin Tool — Geometrical Parameters**

| Parameter | Symbol | Value |
|---|---|---|
| Copper Conductor Radius | R | 0.625 mm |
| Polyimide Enamel Thickness | te | 0.025 mm |
| Outer Radius (Cu + Enamel) | r2 | 0.650 mm |
| Contact Length | L | 5 mm |
| V Angle | α | 90° |
| Applied Normal Force | Fn | 150 N |

**Table 5**
**Tool-Specific Material Parameters**

| Property | Standard Plier (Steel) | Delrin Tool |
|---|---|---|
| Young's Modulus E | 200 GPa | 3.1 GPa |
| Poisson's Ratio ν | 0.29 | 0.35 |

**Table 6**
**Comparison Characteristics**

| Parameter | Steel Plier | Delrin Tool | Reduction |
|---|---|---|---|
| Equivalent Modulus E* | 79.24 GPa | 3.434 GPa | ≦23× more compliant |
| Contact Half-Width b | 17.37 µm | 1,866 µm | Uniform load distribution |
| Max. Hertz Pressure pmax | 1,099 MPa | 5.12 MPa | 99.5% |
| Max. Shear Stress τmax | 334 MPa | 1.56 MPa | ~99.5% |
| Friction Force Ff | 45.0 N | 11.25 N | 75% |
| Bending Moment M | 28.13 N·mm | 7.031 N·mm | 75% |
| Bending Stress σ | 152.7 MPa | 37.87 MPa | 75.2% |
| Safety Factor (enamel) | 0.15 | 4.49 | Enamel protected |
| Safety Factor (copper) | 0.46 | 1.85 | Core protected |

Figure 2 presents the design of the dedicated Delrin forming tool, illustrating the geometry modifications—particularly the contact radius and V-groove profile—that account for the dramatic reduction in peak contact pressure documented in Table 6.

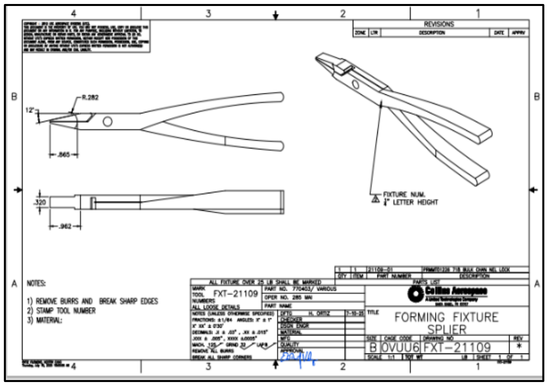


**Figure 2**
**Dedicated Forming Tool Design (Delrin Material)**

The engineering conclusion is clear: replacing the standard steel plier with the Delrin tool effectively eliminates the conditions that lead to enamel insulation failure, providing a safety factor above 4.0 for the enamel layer versus a safety factor below 1.0 for the original tool.

## DESIGN VARIABLES FOR MECHANICAL OPTIMIZATION

The analysis identified four primary mechanical control variables that influenced dielectric failure probability. These variables, summarized in Table 8, form the basis for future tool optimization and process control activities.

**Table 8**
**Key Variables Influencing Dielectric Failure**

| Variable | Impact on System Behavior |
|---|---|
| Contact Radius | Reduces maximum contact pressure |
| Friction Coefficient | Reduces surface abrasion and insulation damage |
| Applied Force | Direct control of mechanical damage severity |
| Surface Roughness | Influences wear and micro-damage generation |

## RESULTS

The combined implementation of mechanical tooling improvements and process standardization produced measurable gains across all tracked quality metrics. Table 9 presents the deliverables assessment, confirming full completion of all five planned corrective actions. Table 10 provides the quantitative performance outcomes against the original targets established at project inception.

**Table 9**
**Deliverables Assessment**

| Deliverable | Before | Target | Final Status |
|---|---|---|---|
| Root Cause Analysis | Not developed | Complete | Completed |
| Standard Work Review (Forming Area) | Not developed | Complete | Completed |
| Process Modification (Tools & Fixtures) | Not existing | Develop/Modify | Implemented |
| Forming Process Training Program | Not existing | Create | Proposed |
| Dielectric Defect Categorization | Not differentiated | Optimize | Optimized |

**Table 10**
**Performance Metrics**

| Metric | Baseline | Target | Final Results |
|---|---|---|---|
| SRR | $200,000 | 35% Reduction | 37% Reduction |
| PPM | 622,042 ppm | 35% Reduction | 30% Reduction |

As shown in Table 10, the SRR target was exceeded (37% vs. 35%), while PPM achieved a 30% reduction. Both outcomes validate the effectiveness of the adopted approach and confirm that tool-driven mechanical damage was indeed the primary source of dielectric defects in this cell.

## CONCLUSION

This project demonstrated that dielectric failures in the Main Stator Cell are primarily driven by mechanical—not electrical—mechanisms. Hertzian contact analysis confirmed that conventional steel pliers generate contact pressures (~1.10 GPa) far exceeding enamel insulation limits, while the dedicated Delrin forming tool reduces this pressure by 99.5%, with corresponding 75% reductions in friction and bending stress.

Complementary process improvements—including standard work updates, dedicated dielectric test operations, improved defect categorization, and operator training—collectively achieved the project's quality and cost targets. The project confirms that tool design and process standardization are decisive factors in dielectric failure prevention for aerospace stator manufacturing.

Future work will focus on:

- Read-Across Analysis for other Main Stator Cell processes.
- Expansion of dielectric failure prevention strategies across additional product families.
- Further optimization of forming tools and operator training programs.
- Integration of predictive quality analytics for early defect detection.

## REFERENCES


[1] K. G. Budinski and M. K. Budinski, Engineering Materials: Properties and Selection, 9th ed. Upper Saddle River, NJ: Pearson Prentice Hall, 2010.

[2] W. D. Callister Jr. and D. G. Rethwisch, Materials Science and Engineering: An Introduction, 10th ed. Hoboken, NJ: Wiley, 2018.

[3] SAE International, "AS9100 Rev D: Quality Management Systems – Requirements for Aviation, Space, and Defense Organizations," SAE International, Warrendale, PA, 2016.

[4] K. L. Johnson, Contact Mechanics. Cambridge, UK: Cambridge University Press, 1985.

[5] M. F. Ashby and D. R. H. Jones, Engineering Materials 1: An Introduction to Properties, Applications and Design, 4th ed. Oxford, UK: Butterworth-Heinemann, 2012.